

# Enhanced performance of pyroelectric microsensors through the introduction of nanoporosity

G. Suyal\*, N. Setter

*Ceramics Laboratory, Federal Institute of Technology, CH-1015 Lausanne, Switzerland*

## Abstract

Sol-gel process has successfully been applied for the deposition of porous  $\text{PbZr}_x\text{Ti}_{1-x}\text{O}_3$  ( $x=0.45, 0.15$ ) thin films on platinized silicon wafers. Addition of a polymer as a volatile phase to the precursor sol prior to spin coating has been proved an excellent method to synthesize PZT-porous films. Introduction of pores creates a matrix void composite resulting in high figures of merit for pyroelectric applications. The dielectric constant was found to be strongly dependent to the porosity, whereas the pyrocoefficient changes moderately with porosity. The relative permittivity can be decreased down to 150 and 95 for PZT films with Zr/Ti ratio of 45/55 and 15/85 respectively, and the figures of merit  $F_V$  and  $F_d$  values for PZT (Zr/Ti = 15/85) films can be increased up to 1.95 and  $139 \mu\text{C}/\text{m}^2 \text{ K}$ , respectively by incorporating a nanoporous structure in films.

© 2003 Elsevier Ltd. All rights reserved.

**Keywords:** Ferroelectric properties;  $\text{Pb}(\text{Zr,Ti})\text{O}_3$ ; Porosity; Sensors; Sol-gel process

## 1. Introduction:

During recent years the use of ferroelectric thin films of  $\text{PbZr}_x\text{Ti}_{1-x}\text{O}_3$  (PZT) family for memory, piezoelectric and pyroelectric<sup>1</sup> devices has drawn considerable interest. These thin films are especially well known candidate materials because of their remarkable ferroelectric properties and stability in device operating ranges.<sup>2–4</sup> The advantage of thin film devices over bulk materials is that they can be directly deposited on platinized silicon to allow direct integration with electronics. The pyroelectric applications of these films those have been commercialized include thermal imaging and gas detection.

To evaluate the quality of a pyroelectric material, different figures of merit exist, depending upon the device requirement. For good voltage response<sup>5</sup> it is necessary to maximize pyrocoefficient  $p$  and lower the permittivity, to increase the figure of merit  $F_V = p/\epsilon_r$ . For high detectivity (signal to noise ratio) the dielectric loss  $\tan \delta$  becomes important and the figure of merit is  $F_d = p/\sqrt{\epsilon_r \tan \delta}$ .<sup>6</sup> One of the possibilities to lower dielectric constant is the incorporation of void space into the films. Seifert et al.<sup>7</sup> have synthesized porous

thin films of  $\text{Pb}_x\text{Ca}_{1-x}\text{TiO}_3$  by controlling the nucleation and growth during rapid thermal annealing of the material. They reported reduced permittivity as low as 55 and a pyrocoefficient as high as  $200 \mu\text{C}/\text{m}^2 \text{ K}$  and related the evolution of the porous structure to the formation of an intermediate Pb–Ca–Ti-fluorite phase before perovskite crystallization. Therefore, this method is only limited to the synthesis of porous PCT films.

It is of interest to develop a general method that will allow the production of uniform films with controlled porosity and which will be applicable also for compositions that do not contain Ca. Therefore, a new method to synthesize porous thin films of PZT has been developed, which has been shown to work also very well with PCT elsewhere.<sup>8</sup>

Chemical solution deposition has been used for the processing of the PZT thin films. The preparation of the PZT organometallic precursor solutions in this work was based on the method reported by Budd et al.<sup>9</sup> Porosity can be introduced in thin films by adding a polymer in the PZT precursor solution prior to spin coating the silicon substrates.

## 2. Experimental procedure

The precursor solution was synthesized from lead acetate trihydrate  $\text{Pb}(\text{CH}_3\text{COO})_2 \times 3.03\text{H}_2\text{O}$  (Fluka),

\* Corresponding author. Tel.: +41-21-693-5869; fax: +41-21-693-5810.

E-mail address: [ganesh.suyal@epfl.ch](mailto:ganesh.suyal@epfl.ch) (G. Suyal).

titanium isopropoxide  $\text{Ti}(\text{OCH}(\text{CH}_3)_2)_4$ , zirconium *n*-propoxide,  $\text{Zr}(\text{OCH}_2\text{CH}_2\text{CH}_3)_4$  and 2-methoxyethanol,  $\text{CH}_3\text{OCH}_2\text{CH}_2\text{OH}$ , (Aldrich Chemie, Buchs-CH).

The solution of 2-methoxyethanol, titanium isopropoxide and zirconium *n*-propoxide was prepared in the glove box. The Ti/Zr solution was added to the lead solution avoiding any contact with air, refluxed for 3 h and then distilled under vacuum to achieve the desired concentration (0.4 M). Resulting solution was cooled down to room temperature and 4 vol.% formamide was added to it in order to improve the drying behavior of the sol-gel.<sup>10</sup> Solutions containing 10 mol% excess Pb were prepared with Zr/Ti ratios of 45/55 and 15/85. Polymers having different molecular weights were added to this sol in different concentrations.

Thin films were deposited using a spin coater (Headway research Inc., Garland, TX, USA) at 3000 rpm for 40 s on in-house platinumized silicon substrates with  $\text{TiO}_2$  adhesion layer between  $\text{SiO}_2$  and Pt. The spin coated films were pyrolyzed for 15 s at 350 °C on a hotplate after each deposition. The substrates containing stacks of four layers were finally heat treated in a rapid thermal anneal apparatus using heating rate of 30 °C/s.

Field emission scanning electron microscopy (SEM; Jeol, 6300 F Tokyo Japan, and Philips) and X-ray diffraction (XRD, Siemens, D500, Munich, Germany) were used for micro-structural characterization of the films. For electrical characterization circular Au top electrodes of 0.6 mm diameter were deposited by evaporation through a shadow mask. Profilometer thickness measurements ( $\alpha$ -step 260, Tencore, Mountain View, CA, USA) and bottom electrode contact were facilitated by etching a part of PZT layer in a HF/HCl/ $\text{H}_2\text{O}$  mixture.

A multi frequency LCR-meter (Hewlett Packard 4274A, Palo Alto, CA, USA) was used to determine dielectric loss,  $\tan \delta$ , and to measure capacitance in order to calculate permittivities of the films. Pyroelectric currents were measured dynamically as a function of a 1 K temperature change, controlled by a wave-form generator driven peltier element.<sup>11</sup> In order to achieve high pyrocoefficient  $p$ , the films were poled on a hotplate for 10 min at the temperatures of 150–200 °C and the fields of 200–700 kV/cm. The poling field necessary to achieve an optimized pyrocoefficient was determined experimentally by systematically increasing the field strength and temperature until no further improvement of  $p$  could be measured.

### 3. Results and discussion

The SEM micrographs of thin films synthesized by the solutions containing 10% of high and low molecular weight polymers are shown in Fig. 1. These micrographs show that the films contain a nice porous structure. The

SEM micrographs of thin films containing 10% of high molecular weight polymer are shown in Fig. 1(a)–(c). It can clearly be seen from Fig. 1(a) that the surface contains some cracks, but in spite of these cracks the electric properties were not deteriorated. Fig. 1(b) shows the SEM image of the same sample at higher magnification. Whereas, the cross sectional view of the porous film is shown in Fig. 1(c), which shows that there are no pores going from the top to the bottom of the films. The SEM image of thin films containing 10% of low molecular weight polymer is shown in Fig. 1(d). Final thickness of the films containing high and low molecular weight polymers was measured to be equal to 1.4  $\mu\text{m}$  and 0.9  $\mu\text{m}$  respectively, by SEM and profilometry both.

#### 3.1. X-ray diffraction characterization

X-ray diffraction patterns of both the samples containing low and high molecular weight polymer and annealed at 650 °C for 10 min, and a sample pyrolysed at 350 °C for 15 s are shown in Fig. 2. This figure clearly shows that after pyrolysing at 350 °C material remains amorphous only, and no diffraction peak corresponding to perovskite phase was observed. Whereas, for the samples annealed at 650 °C for 10 min, all the diffraction peaks corresponding to (100) (101) (111) planes of PZT were obtained. These observations confirm that for porous PZT no preferred orientation was observed.

#### 3.2. Electric characterization

For the electrical characterization,  $\epsilon_r$ ,  $\tan \delta$  and  $p$  were measured before and after poling of PZT thin films. The dielectric losses at 1 kHz for porous films were  $\tan \delta = 0.020$ – $0.025$ . Low  $\epsilon_r$  results from porous films for example, 150 for porous PZT, whereas it is as much as 800 for dense PZT films. Lichtenecker's rule gives the permittivity for a mixture  $\epsilon_m$  of dielectric phases with mixed series and parallel connectivity.<sup>5</sup> Using the measured permittivity of the porous films as  $\epsilon_m$ , the permittivity of dense films as  $\epsilon_1$ , and the dielectric constant of air for the pores in films as  $\epsilon_2 = 1$ , the volume fraction  $V_2$  of the porosity can be calculated equal to 20 and 25% for the films having low and high molecular weight polymer respectively, using the equation " $\ln \epsilon_m = V_1 \ln \epsilon_1 + V_2 \ln \epsilon_2$ ".

Poling experiments were carried out to find the lowest possible temperature and electric field strength to achieve a maximum pyroelectric coefficient. The development of  $p$  and  $\epsilon_r$  for PZT samples containing different molecular weight polymers is shown in Fig. 3(a). The samples were poled for 10 min at a constant temperature of 150 °C. This figure shows that the increase in poling field decreases the permittivity and increases the pyrocoefficient. For the samples having higher porosity, the increase in the poling field from 100 to 500 kV/cm

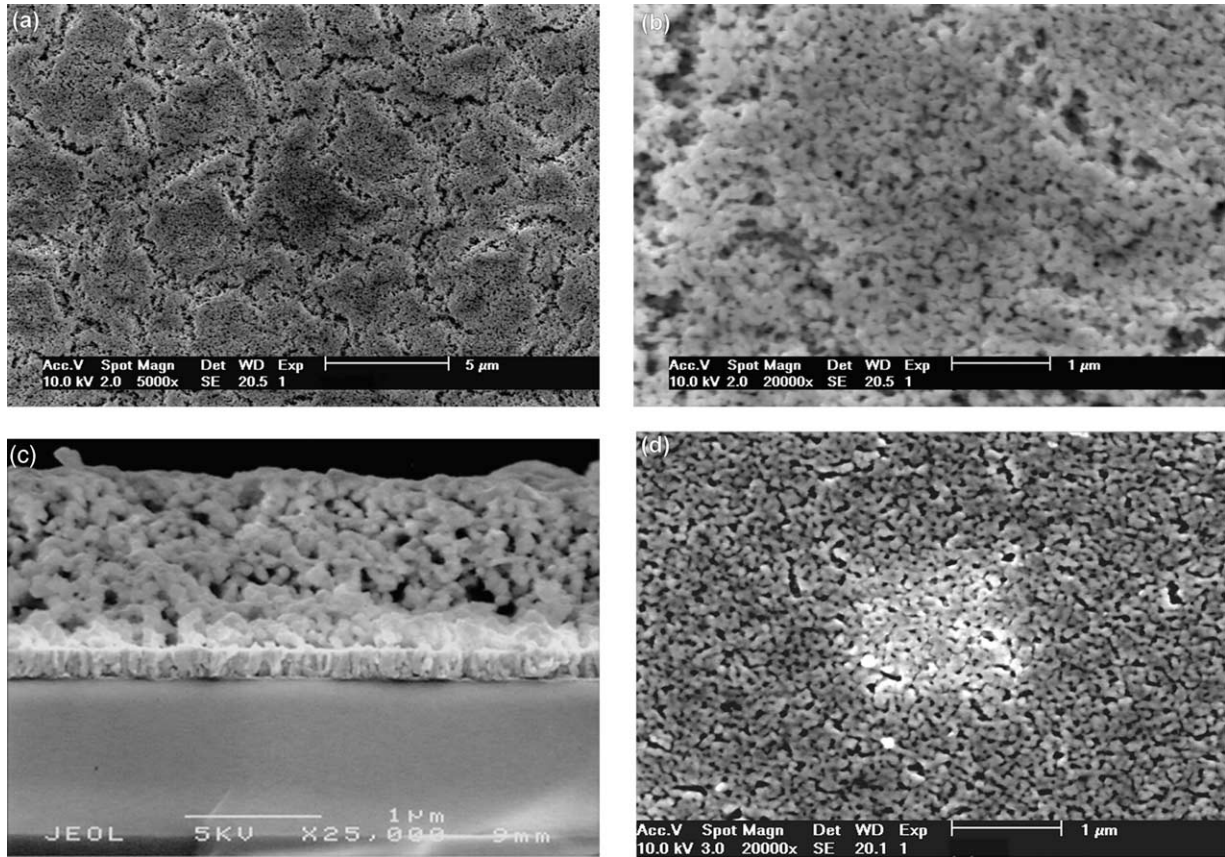


Fig. 1. SEM micrographs of porous PZT films containing 10% polymer (a) high molecular weight polymer: (b) higher magnification, (c) cross sectional view, (d) low molecular weight polymer.

increases the pyrocoefficient from 86 to 120  $\mu\text{C}/\text{m}^2 \text{ K}$ , and the relative permittivity decreases from 156 to 127. Whereas, for the samples with relatively lower porosity, the increase of poling field from 100 to 700 kV/cm

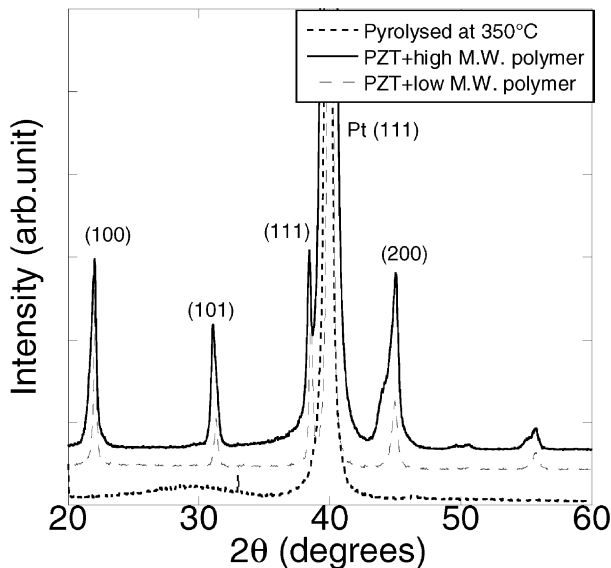


Fig. 2. X-ray diffraction patterns of porous PZT thin films.

increases the pyrocoefficient from 65 to 145  $\mu\text{C}/\text{m}^2 \text{ K}$  and decreases the permittivity from 202 to 145.

For the samples containing high molecular weight polymer, the relative permittivity is less than the sample containing low molecular weight polymer, but the samples did not show a high pyrocoefficient, which is also essential in order to get high figures of merit. On comparing the pyrocoefficient of two samples having different porosities, it can be observed that the maximum pyrocoefficient for the films having higher porosity was measured lower (120  $\mu\text{C}/\text{m}^2 \text{ K}$ ) than the pyrocoefficient for the films with lower porosity (147  $\mu\text{C}/\text{m}^2 \text{ K}$ ). This behavior can be explained by the fact that the films with higher porosity will have a proportionally reduced charge density and hence a reduced pyrocoefficient. The dielectric strength of the films must have played a role as well, since the more porous film could not withstand a higher field than 500 kV/cm, perhaps the saturation of polarization has not been achieved. Therefore, only the low molecular weight polymer was used for further studies.

The voltage ( $F_v$ ) and detectivity ( $F_d$ ) figures of merit as a function of poling field, for two PZT samples containing high M.W. (estimated porosity 25%) and low M.W. (estimate porosity 20%) polymer are shown in

Fig. 3(b). The maximum values of  $F_v$  and  $F_d$  were calculated about 0.98 and 80  $\mu\text{C}/\text{m}^2\text{K}$  for the films containing high M.W. polymer, whereas, those for the films containing low M.W. polymer were calculated equal to 1.1 and 80  $\mu\text{C}/\text{m}^2\text{K}$ , respectively.

It is known from the literature that the permittivity of the thin films has often been found to peak at the PZT composition near the morphotropic phase boundary. Therefore, in order to maximize the figures of merit  $F_v$  and  $F_d$ , useful composition of  $\text{PbZr}_x\text{Ti}_{1-x}\text{O}_3$  will be corresponding to the  $x$  equal to 15%, because this composition offers comparatively low dielectric constant as desired. Therefore, samples were prepared by mixing 10% of low molecular weight polymer to the PZT sol having Zr/Ti ratio of 15/85. Fig. 4(a) shows the

pyrocoefficient and permittivity as a function of poling field for PZT (15/85) samples. This figure shows that for PZT porous films, on increasing the poling field from 100 to 700 kV/cm the permittivity decreases from 142 to 91, whereas, the pyroelectric coefficient increases from 70 to 180  $\mu\text{C}/\text{m}^2\text{K}$ . The figures of merit  $F_v$  and  $F_d$  for these samples are shown in Fig. 4(b). The  $F_v$  and  $F_d$  values can be increased to 1.95 and 135  $\mu\text{C}/\text{m}^2\text{K}$ , respectively for porous PZT films, whereas, these values are 0.88 and 80  $\mu\text{C}/\text{m}^2\text{K}$ , respectively, for dense PZT films.

The relative permittivity, the maximum measured pyroelectric coefficient, and the calculated figures of merit  $F_v$  and  $F_d$  of the dense- and porous- $\text{PbZr}_x\text{Ti}_{1-x}\text{O}_3$  ( $x=0.45$  and 0.15) samples are given in Table 1.

The polarization hysteresis loops of PZT dense- and porous-films showed that the porous PZT films are very hard to pole as compared to dense PZT films and relatively a high poling field is required (almost double to that required for dense PZT films) for the poling of

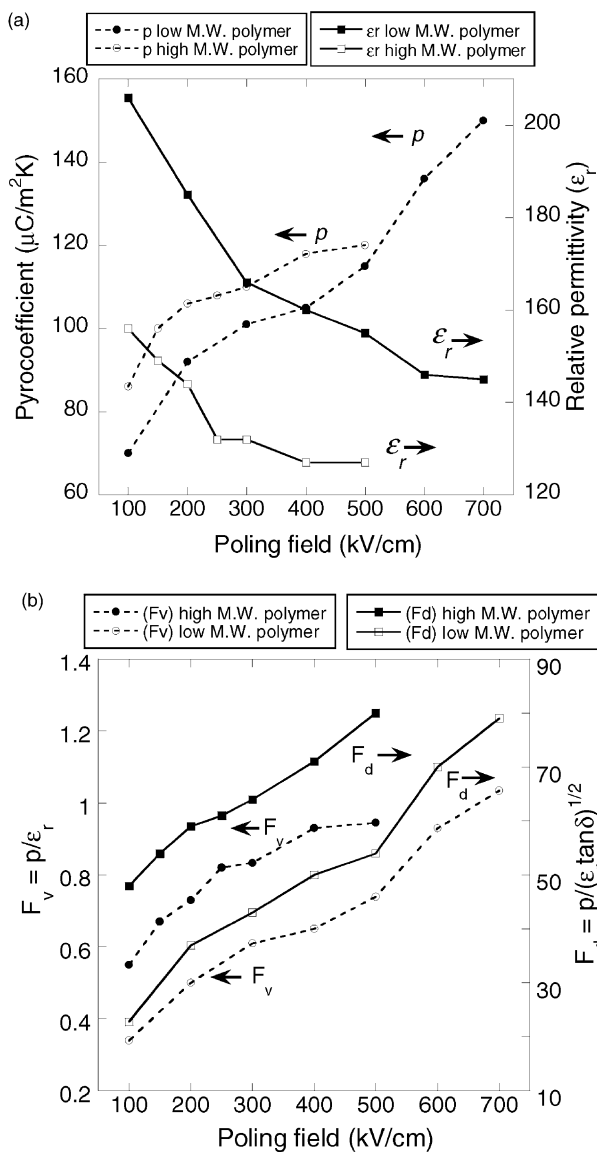


Fig. 3. Influence of poling field on (a) pyrocoefficient and permittivity of porous PZT (Zr/Ti = 45/55) films, containing low and high molecular weight polymers, (b) their figures of merit ( $F_v$ ) and ( $F_d$ ).

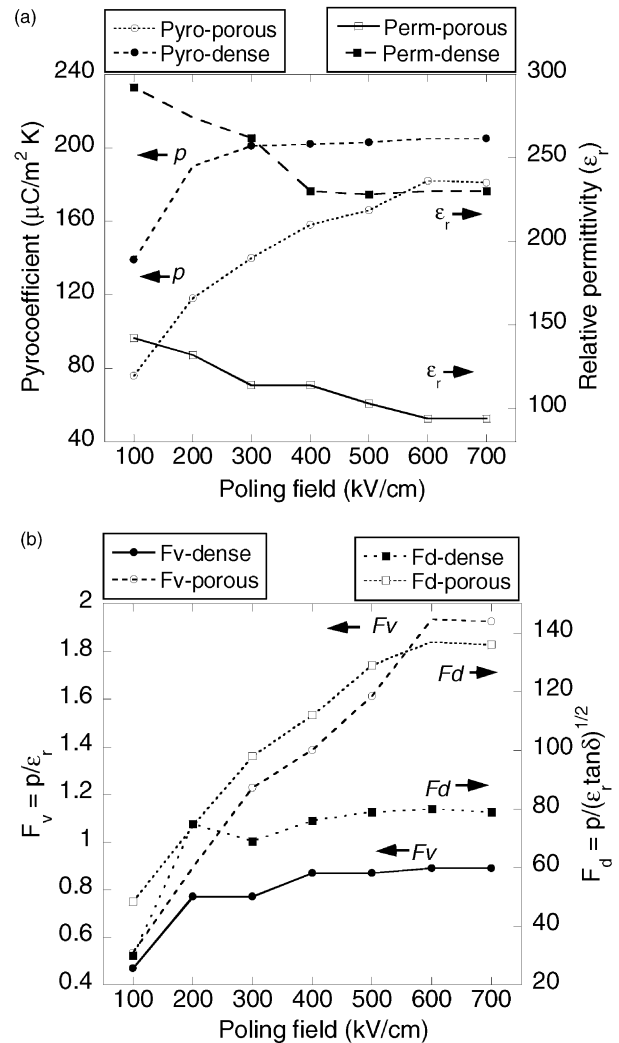


Fig. 4. (a) Pyrocoefficient and permittivity of porous- and dense-PZT (Zr/Ti = 15/85) films, as a function of poling field, (b) figures of merit ( $F_v$ ) and ( $F_d$ ).

Table 1  
Electrical parameters of the porous- and dense-PZT (Zr/Ti = 45/55, 15/85) films

	Estimated porosity (%)	$\epsilon_r$ before poling	$\epsilon_r$ after poling <sup>a</sup>	$p$ ( $\mu\text{C}/\text{m}^2\text{K}$ )	$F_v$ ( $\mu\text{C}/\text{m}^2\text{K}$ )	$F_d$ ( $\mu\text{C}/\text{m}^2\text{K}$ )
Dense PZT (45/55)	–	870	784	215	0.28	38
High M.W. polymer <sup>b</sup>	25	156	127	119	0.94	79
Low M.W. polymer <sup>b</sup>	21	206	144	150	1.00	80
Dense PZT (15/85)	–	300	230	205	0.88	79
Low M.W. polymer <sup>c</sup>	20	142	91	180	1.92	139

<sup>a</sup> Poling at 150 °C, 700 KV/cm.

<sup>b</sup> PZT (Zr/Ti = 45/55).

<sup>c</sup> PZT (Zr/Ti = 15/85).

porous films. It may be due to the small grain size of about 50 nm for porous PZT. Domain wall motion and thus polarizability is known to be significantly reduced in small grained materials.<sup>12,13</sup>

#### 4. Conclusions

In conclusion, porous pyroelectric thin films of PZT have successfully been synthesized by incorporating a polymer to the precursor solution synthesized by sol-gel route. The use of a polymer as a volatile phase has been proved to be an excellent method for introducing a porous microstructure in PZT films. It has been shown that the pore volume can easily be controlled by changing the molecular weight and the concentration of the polymer used. For PZT (Zr/Ti = 45/55) the  $F_v$  and  $F_d$  values were increased from 0.28 to 1.0  $\mu\text{C}/\text{m}^2\text{K}$  and 38 to 80  $\mu\text{C}/\text{m}^2\text{K}$ , respectively, whereas for  $\text{PbZr}_{0.15}\text{Ti}_{0.85}\text{O}_3$  these values were increased from 0.88 to 1.95  $\mu\text{C}/\text{m}^2\text{K}$  and 79 to 139  $\mu\text{C}/\text{m}^2\text{K}$ , respectively, by introducing a porous microstructure.

#### References

1. Kohli, M., Wuethrich, C., Brooks, K., Willing, B., Forser, M., Muralt, P., Setter, N. and Ryser, P., *Sensor and Actuator*, 1997, **A60**, 147.
2. Paz de Araudjo, C. A., Cuchiario, J. D., McMillan, L. D., Scott, M. C. and Scott, J. F., *Nature*, 1995, **74**, 627.
3. Chen, J., Harmer, M. J. and Smyth, D. M., *J. App. Phys.*, 1994, **76**, 5394.
4. Warren, W. L., Dimos, D., Tuttle, B. A., Nasby, R. D. and Pike, G. E., *App. Phys. Let.*, 1994, **65**, 1018.
5. Moulson, A. J. and Herbert, J. M., *Electroceramics*. Chapman and Hall, London, 1990.
6. Muralt, P., *Revue de l'électricité de de l'électronique*, 1996, **9**, 56.
7. Seifert, A., Sagalowicz, L., Muralt, P. and Setter, N., *J. Mat. Res.*, 1999, **14**, 2012.
8. Suyal, G., Seifert, A. and Setter, N., *App. Phys. Let.*, 2002, **81**(6), 1059.
9. Budd, K. D., Dey, S. K. and Payne, D. A., *British Ceramics Proceedings*, 1985, **36**, 107.
10. Ortel, G. and Hench, L., *J. of Non-Cry. Sol.*, 1986, **79**, 177.
11. Hartley, N. P., Squire, P. T. and Putley, E. H., *J. Phys.*, 1972, **E5**, 787.
12. Arlt, G., *Ferroelectrics*, 1987, **76**, 451.
13. Arlt, G. and Pertsev, N. A., *J. App. Phys.*, 1991, **70**, 2283.